

# Gi-coupled receptor activation potentiates Piezo2 currents via G $\beta\gamma$

John Smith Del Rosario<sup>1</sup>, Yevgen Yudin<sup>1</sup>, Songxue Su<sup>1</sup>, Cassandra M Hartle<sup>2</sup>, Tooraj Mirshahi<sup>2</sup>  & Tibor Rohacs<sup>1,\*</sup> 

## Abstract

Mechanically activated Piezo2 channels are key players in somatosensory touch, but their regulation by cellular signaling pathways is poorly understood. Dorsal root ganglion (DRG) neurons express a variety of G-protein-coupled receptors that modulate the function of sensory ion channels. Gi-coupled receptors are generally considered inhibitory, as they usually decrease excitability. Paradoxically, activation of Gi-coupled receptors in DRG neurons sometimes induces mechanical hypersensitivity, the mechanism of which is not well understood. Here, we find that activation of Gi-coupled receptors potentiates mechanically activated currents in DRG neurons and heterologously expressed Piezo2 channels, but inhibits Piezo1 currents in heterologous systems in a G $\beta\gamma$ -dependent manner. Pharmacological inhibition of kinases downstream of G $\beta\gamma$ , phosphoinositide 3-kinase (PI3K) and mitogen-activated protein kinase (MAPK) also abolishes the potentiation of Piezo2 currents. Local injection of sumatriptan, an agonist of the Gi-coupled serotonin 1B/1D receptors, increases mechanical sensitivity in mice, and the effect is abolished by inhibiting PI3K and MAPK. Hence, our studies illustrate an indirect mechanism of action of G $\beta\gamma$  to sensitize Piezo2 currents and alter mechanosensitivity after activation of Gi-coupled receptors.

**Keywords** Gi-coupled receptors; G-protein  $\beta\gamma$ ; MAPK; PI3K; Piezo2

**Subject Categories** Membrane & Trafficking; Neuroscience

**DOI** 10.15252/embr.201949124 | Received 21 August 2019 | Revised 26

February 2020 | Accepted 6 March 2020 | Published online 29 March 2020

**EMBO Reports (2020) 21: e49124**

## Introduction

Our ability to sense environmental cues is vital for our daily activities. Our tactile world relies on a wide variety of mechanosensory neurons that innervate our skin and are responsible for sensing innocuous and painful stimuli attributed to low-threshold mechanoreceptors (LTMRs) and nociceptors, respectively. These neurons detect external mechanical stimuli and convert them into

ionic currents using mechano-gated ion channels, including the excitatory Piezo2 non-selective cation channels and the inhibitory K<sup>+</sup> selective TREK1 and TREK2 channels [1,2]. Piezo2 channels are intrinsically gated by force and mediate rapidly adapting mechanically activated (MA) currents in dorsal root ganglion (DRG) neurons and when heterologously expressed. Reports have shown that Piezo2 channels play a pivotal role in the detection of light touch, proprioception, and mechanical pain in mice and humans [3–9]. In addition, these channels are essential regulators of embryonic development, lung expansion, reverse polarity currents of auditory hair cells, Merkel cell mechanotransduction, baroreception, and itch [10–15]. Despite the substantial progress in describing the physiological importance of Piezo2, little is known about how endogenous signaling pathways modulate the activity of these channels.

Dorsal root ganglion neurons express a wide variety of G-protein-coupled receptors. Gs- and Gq-coupled receptors generally increase excitability of DRG neurons, and many of them are activated by inflammatory mediators such as prostaglandins and bradykinin. Activation of the Gq-coupled bradykinin receptor B2 was shown to sensitize Piezo2 currents in heterologous systems and in DRG neurons through a mechanism involving the activation of PKA and PKC, an effect that may play a role in inflammatory mechanical allodynia [16].

Whether the activation of Gi-coupled receptors influences the activity of Piezo2 channels has not been studied yet. Activation of Gi-coupled receptors leads to inhibition of adenylate cyclase, activation of G-protein-coupled inwardly rectifying K<sup>+</sup> (GIRK) channels, and inhibition of voltage-gated Ca<sup>2+</sup> channels (VGCC) and of transient receptor potential melastatin 3 (TRPM3) channels in DRG neurons through direct binding of G $\beta\gamma$  [17–21]. In addition, G $\beta\gamma$  is also known to induce the activation of phosphoinositide 3-kinase gamma (PI3K) and mitogen-activated protein kinase (MAPK) enzymes [22–25].

Many different Gi-coupled receptors, such as GABA<sub>B</sub>, and opioid receptors are expressed in DRG neurons; their activation generally reduces excitability and exerts analgesic effects [26]. Activation of many Gi-coupled receptors however was also shown to induce mechanical hypersensitivity, the mechanism of which is not well understood [26–28].

<sup>1</sup> Department of Pharmacology, Physiology and Neuroscience, New Jersey Medical School, Rutgers, the State University of New Jersey, Newark, NJ, USA

<sup>2</sup> Department of Molecular and Functional Genomics, Weis Center for Research, Geisinger Clinic, Danville, PA, USA

\*Corresponding author. Tel: +1 973 972 4464; E-mail: rohacsti@njms.rutgers.edu

Here, we found that activation of Gi-coupled receptors potentiated native MA currents in DRG neurons and the activity of heterologously expressed Piezo2 channels in HEK293 cells without affecting the number of channels at the plasma membrane. Surprisingly, the currents of the closely related Piezo1 channels were inhibited after activation of Gi-coupled receptors in HEK293 cells. The potentiation of Piezo2 and inhibition of Piezo1 currents were abolished when blocking  $G\beta\gamma$ . Furthermore, inhibition of PI3K and MAPK also abolished the potentiation of Piezo2 currents. Our behavioral studies also show that local injection of sumatriptan an agonist of the Gi-coupled serotonin 1B/1D (Htr1b and Htr1d) receptors increased sensitivity to mechanical stimuli using von Frey filaments, an assay that was shown to depend on Piezo2 channels [3]. This increase in mechanosensitivity was also abolished when blocking PI3K and MAPK enzymes. In conclusion, our data show that activation of Gi-coupled receptors potentiates Piezo2 currents and Piezo2-mediated touch sensitivity through a mechanism potentially involving a  $G\beta\gamma$ -dependent PI3K and MAPK activation.

## Results and Discussion

### GABA<sub>B</sub> receptor activation potentiates native MA currents in DRG neurons

At the RNA level, GABA<sub>B</sub> receptors are the highest expressing Gi-coupled receptors in DRG neurons [29,30]. Therefore, we tested if activation of GABA<sub>B</sub> receptors could influence the activity of MA currents in DRG neurons. We mechanically stimulated, with a blunt glass probe, large diameter DRG neurons (cell capacitance > 40 pF), which are most likely mechanoreceptors [31], and correspond to the NF1-NF5 neuronal population, which expresses Piezo2 at the RNA level in ~90% of the cells [30]. First, we repetitively applied short mechanical stimuli of the same amplitude every 30 s, and we activated GABA<sub>B</sub> receptors by applying 25  $\mu$ M baclofen. Baclofen application potentiated MA currents in 50% of neurons tested (Fig 1B and C). In control experiments, neurons treated with vehicle only, we did not observe current potentiation (Fig 1A and C).

We also measured MA currents using a 2–6  $\mu$ m step protocol, in which we increased the displacement of the glass probe every 15 s by 0.4  $\mu$ m. After recording the basal MA currents, the cells were treated with 25  $\mu$ M baclofen for 3 min and MA currents were re-recorded for comparison in the continuous presence of baclofen. As expected, activation of GABA<sub>B</sub> receptors also potentiated MA currents almost twofold (Fig 1D–F) in 59% of the neurons and had no effect in 41% of DRG neurons tested (Fig 1G) probably because not every DRG neuron co-expresses GABA<sub>B1</sub> and GABA<sub>B2</sub> receptors and the obligatory heterodimerization of these receptors is required for proper G-protein signaling [26,32]. In both protocols, baclofen-induced potentiation was long lasting and persisted for several minutes after removal of the agonist (Fig 1B, C and F, dashed line).

The kinetics of inactivation of responding cells was somewhat slower after baclofen application (Fig 1H), but not in neurons that did not respond to baclofen with an increase in current amplitude (Fig 1I). Approximately 36% of the neurons we tested responded to mechanical stimulation with transient inward currents; the average

inactivation time constant was  $18.10 \pm 1.61$  ms in baclofen responsive neurons and  $20.86 \pm 1.91$  ms in baclofen non-responsive neurons. In all responsive neurons, the currents decayed to zero by the end of the 200-ms mechanical stimulation.

Dorsal root ganglion neurons display MA currents with different inactivation kinetics that are usually categorized as rapidly adapting (RA), intermediate adapting (IA), and slowly adapting (SA), with RA currents displayed in more than 50% of the neurons responding to mechanical stimulation [3]. Piezo2 has been shown to mediate RA currents, and currently, there is no knowledge on the molecular counterparts of IA and SA currents. The average inactivation time constant of MA currents in our experiments in DRG neurons is similar to the inactivation time constant of RA currents in DRG neurons in our earlier study [33], but it is slower than the < 10 ms used in other publications for example in reference [1]. The inactivation time constant of both recombinant Piezo2 [34,35] and Piezo1 currents [35,36] shows substantial variability between different studies. The finding that the inactivation time constant of MA currents in DRG neurons and in HEK cells transfected with Piezo2 (see next paragraph) was very similar in our experiments suggests that most MA currents we recorded in DRG neurons were mediated by Piezo2. It cannot be excluded, however, that other MA channels in some neurons contributed to the responses to baclofen or that other MA channels were responsible for lack of responsiveness to receptor stimulation in some neurons.

### GABA<sub>B</sub> receptor activation potentiates Piezo2 currents in a heterologous system

To determine whether the potentiation of MA currents was specific to Piezo2 channels, we co-expressed Piezo2 and GABA<sub>B1</sub> and GABA<sub>B2</sub> receptors in HEK293 cells. Using the same step protocol as in DRG neurons, we recorded Piezo2 currents in these cells (Fig 2). Similar to DRG neurons, the currents evoked in Piezo2-transfected HEK293 cells fully decayed by the end of the 200-ms mechanical stimulation, with an inactivation time constant of  $18.5 \pm 1.2$  ms (Fig 2D), which is very similar to that we observed in DRG neurons (Fig 1H and I). In HEK293 cells transfected with GFP only, the same mechanical stimulation did not evoke any currents (Fig EV1), which indicates that the MA currents we measured in Piezo2-transfected HEK293 cells were mediated by Piezo2.

When we applied the GABA<sub>B</sub> receptor agonist baclofen (25  $\mu$ M) for 3 min, and re-recorded MA currents in the continuous presence of the drug, Piezo2 current amplitudes increased approximately twofold (Fig 2A–C). There was no statistically significant difference in the kinetics of inactivation of Piezo2 currents after baclofen application (Fig 2D). Piezo2 currents recorded from HEK293 cells transfected with only Piezo2 were not potentiated by baclofen treatment, showing that baclofen exerted its potentiating effect via the activation of GABA<sub>B</sub> receptors (Fig 2E).

### GABA<sub>B</sub> receptor activation potentiates Piezo2 currents via $G\beta\gamma$

Activation of Gi-coupled receptors leads to dissociation of the G-proteins  $G\alpha_i$  and  $G\beta\gamma$ . The  $G\alpha_i$  subunit inhibits adenylate cyclase, while  $G\beta\gamma$  inhibits neuronal activity through activation of GIRK channels [37] and VGCC [38]. To test whether Piezo2 potentiation

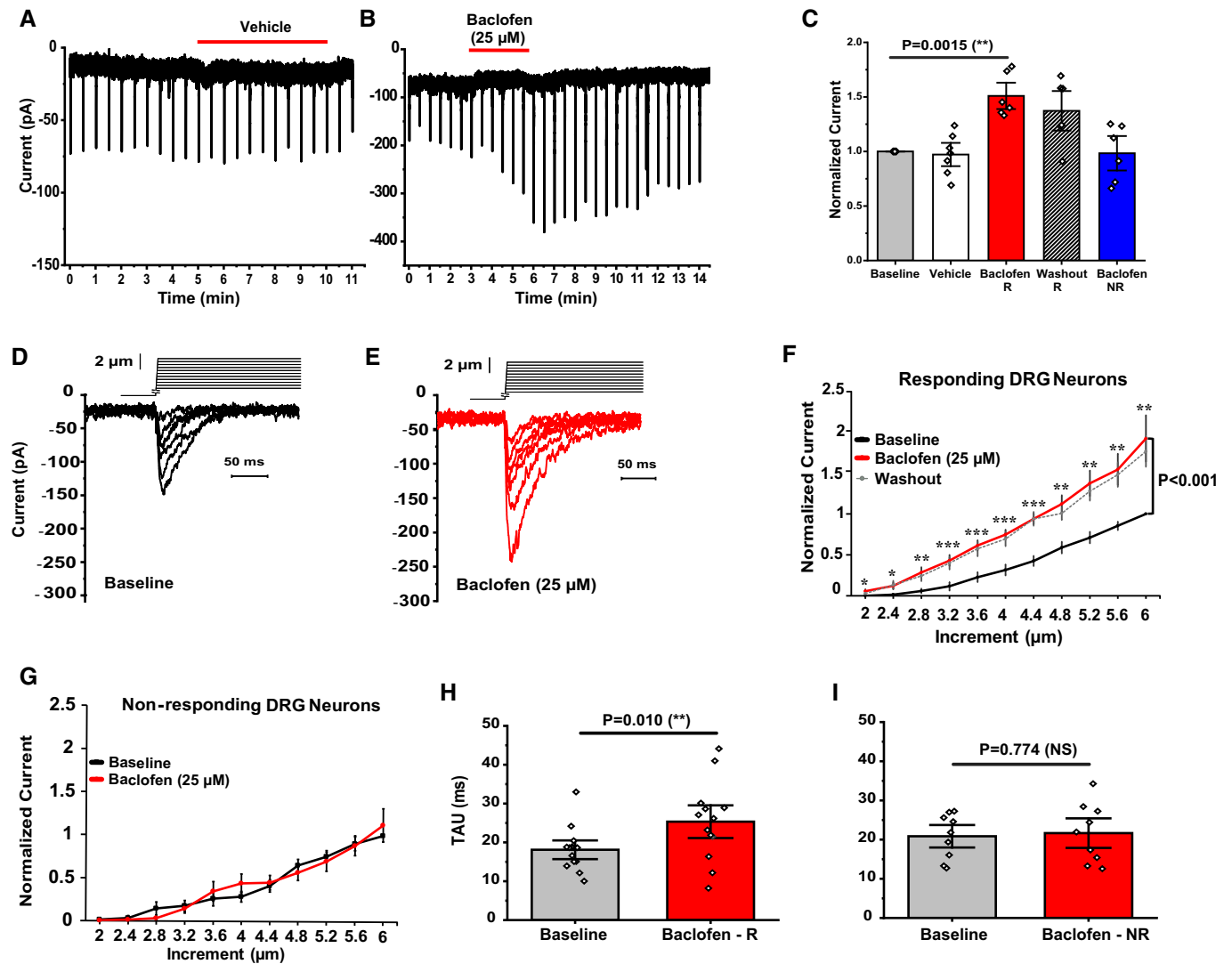


**Figure 1. GABA<sub>B</sub> receptor activation potentiates MA currents in DRG neurons.**

A, B Representative MA currents recorded in whole-cell patch-clamp experiments at  $-60$  mV in large DRG neurons in response to repetitive mechanical indentations with a blunt glass probe; experiments were performed as described in the Materials and methods section. The applications of  $25 \mu\text{M}$  baclofen (B) or vehicle (A) are indicated by the red horizontal lines. The downward spikes represent individual MA currents induced by repetitive,  $200$  ms long mechanical stimuli every  $30$  s.

C Quantification of normalized MA current amplitudes from DRG neurons, vehicle (white,  $n = 7$ ), neurons responding to baclofen (R, red;  $n = 6$ ,  $**P < 0.01$ , paired  $t$ -test), and non-responding DRG neurons (NR, blue,  $n = 6$ ). Striped column shows the average normalized current amplitudes  $3$ – $10$  min after removal of baclofen in responding neurons (washout;  $n = 6$ ). Data are shown as mean  $\pm$  SEM and scatter plots.

D, E Representative MA currents recorded at  $-60$  mV in large DRG neurons in response to repetitive mechanical stimulation with a blunt glass probe displaced  $2$ – $6 \mu\text{m}$  in  $0.4$ - $\mu\text{m}$  increments every  $15$  s (step protocol) before (black) and after (red) exposure to  $25 \mu\text{M}$  Baclofen. Not every trace is shown for clarity. Inset above the current traces shows the mechanical step protocol indicating the displacement of the mechanical probe.

F Quantification of normalized MA currents of responding large DRG neurons ( $n = 13$ ,  $*P < 0.05$ ,  $**P < 0.01$ ,  $***P < 0.001$ ) before (black) and after (red) baclofen treatment. Dashed gray line shows average MA currents  $3$ – $15$  min after washout of baclofen. Repeated-measures ANOVA with Student's  $t$ -test no corrections was used to compare baseline and baclofen treatment. Data are shown as mean  $\pm$  SEM.

G Quantification of normalized MA currents of non-responding DRG neurons ( $n = 9$ ). Data are shown as mean  $\pm$  SEM.

H, I Quantification of MA current inactivation rate (Tau) measured for responding (R) large DRG neurons ( $n = 13$ ,  $**P < 0.01$ , paired  $t$ -test) and non-responding (NR) large DRG neurons ( $n = 9$ , NS, not significant) before (gray) and after (red) baclofen application. Data are shown as mean  $\pm$  SEM and scatter plots.

requires  $G\beta\gamma$ , we co-transfected HEK293 cells with Piezo2 channels, GABA<sub>B</sub> receptors, and the c-terminal domain of the  $\beta$ -adrenergic receptor kinase ( $\beta\text{ARKct}$ ), which is known to block the effects of  $G\beta\gamma$  [19,38]. Co-transfection of  $\beta\text{ARKct}$  abolished the potentiation of Piezo2 currents after activation of GABA<sub>B</sub> receptors by baclofen (Fig 2F), indicating the involvement of  $G\beta\gamma$ .

#### Activation of other Gi-coupled receptors also potentiates MA currents in DRG neurons and Piezo2 currents in a heterologous system

Next, we tested whether potentiation of Piezo2 currents was caused by a general Gi-coupled receptor mechanism, or one specific to

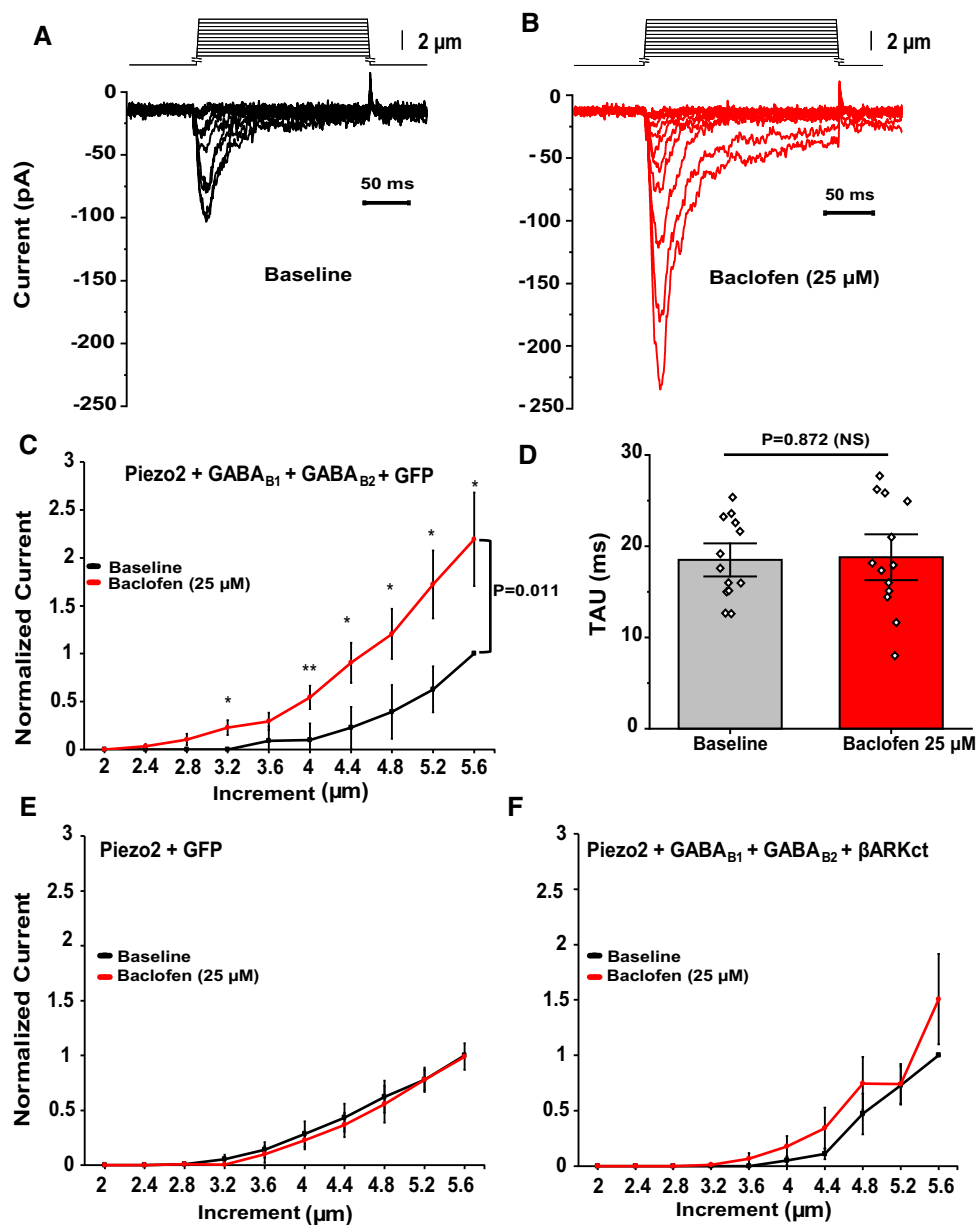


**Figure 2. GABA<sub>B</sub> receptor activation potentiates Piezo2 currents in a heterologous system via Gβγ.**

- A, B Representative MA currents recorded in whole-cell patch-clamp experiments at -60 mV in HEK293 cells transiently transfected with Piezo2 + GABA<sub>B1</sub> + GABA<sub>B2</sub> + GFP (for visualization) in response to repetitive mechanical stimulation with a blunt glass probe displaced 2–5.6 μm in 0.4-μm increments every 15 s before (black) and after (red) exposure to 25 μM baclofen. Not every trace is shown for clarity.
- C Quantification of normalized MA currents of HEK293 cells transfected with Piezo2 + GABA<sub>B1</sub> + GABA<sub>B2</sub> + GFP ( $n = 13$ , \* $P < 0.05$ , \*\* $P < 0.01$ , before [black] and after [red] baclofen treatment, repeated-measures ANOVA with Student's  $t$ -test no corrections). Data are shown as mean  $\pm$  SEM.
- D Quantification of MA current inactivation rate (Tau) in HEK293 cells transfected with Piezo2 + GABA<sub>B1</sub> + GABA<sub>B2</sub> + GFP before (gray) and after (red) baclofen application ( $n = 13$ , NS, not significant; paired  $t$ -test). Data are shown as mean  $\pm$  SEM and scatter plots.
- E, F Quantification of normalized MA currents of HEK293 cells transfected with Piezo2 + GFP (E,  $n = 7$ ) and Piezo2 + GABA<sub>B1</sub> + GABA<sub>B2</sub> + βARKct-mCherry (F,  $n = 8$ ) before (black) and after (red) application of 25 μM baclofen. Data are shown as mean  $\pm$  SEM.

GABA<sub>B</sub> receptors, as it was reported for the inhibition of the sensitized state of TRPV1 channels [39]. We transfected HEK293 cells with Piezo2 channels and the Gi-coupled D2 dopamine receptors, and we found that the D2/D3 agonist quinpirole (200 nM) potentiated Piezo2 currents (Fig 3A). Cells transfected with only Piezo2 did

not show any MA current potentiation after quinpirole treatment (Fig 3B), indicating the role of D2 receptor activation. Quinpirole had no effect on the inactivation time constant of Piezo 2 current (Fig 3C). These findings imply that the effect of Piezo2 current potentiation is a general Gi-coupled receptor-dependent mechanism.

Our ability to reconstitute Gi-coupled receptor potentiation of Piezo2 in a heterologous system also indicates that the effect does not depend on DRG neuron-specific proteins, rather it is mediated by Gi-signaling pathway components, which are present in HEK293 cells.

The Gi-coupled serotonin receptor 1D (Htr1d) is also highly expressed in large diameter DRG neurons [30]. We measured MA currents from these DRG neurons and treated them with 10  $\mu$ M of sumatriptan an agonist of Htr1d and Htr1b serotonin receptors, a clinically used medication against migraine. Sumatriptan potentiated MA currents in 63% of DRG neurons, while in 37% of the neurons it did not (Fig 3D and E). Sumatriptan induced a small increase in the inactivation time constant of MA currents, but this effect did not reach statistical significance (Fig 3F).

It was reported that on the RNA level 71% of the large NF1-NF5 DRG neurons co-express Htr1d and Piezo2 and 41.7% co-express Piezo2 and GABA<sub>B1</sub> and GABA<sub>B2</sub> receptors [30]. The NF1-NF5 cell population likely corresponds to the large neurons we patched, and the numbers are comparable with the responsiveness of the neurons to baclofen and sumatriptan in our work.

To test whether G $\beta$  $\gamma$  is sufficient for potentiation, we introduced G $\beta$  $\gamma$  into the intracellular solution in the whole-cell patch pipette and measured MA currents in DRG neurons immediately after establishment of the whole-cell mode and 6 min later. MA currents were significantly enhanced after 6 min in neurons dialyzed with G $\beta$  $\gamma$  (Fig 3G), but not in neurons where G $\beta$  $\gamma$  was omitted from the patch pipette solution (Fig 3H). The inactivation time constant at the end of the experiment was higher than the one measured at the beginning in neurons dialyzed with G $\beta$  $\gamma$  (Fig 3I), but not in neurons without G $\beta$  $\gamma$  (Fig 3J).

These data indicate that G $\beta$  $\gamma$  is sufficient to modulate the activity of Piezo2 currents. While the contribution of G $\alpha$ i-dependent mechanisms cannot be excluded, their involvement is unlikely as G $\alpha$ i is known to inhibit the activity of adenylate cyclase, an enzyme that induces potentiation of Piezo2 currents when activated by inflammatory mediators [16].

The inactivation time constant became longer after baclofen treatment in DRG neurons (Fig 1H), but not in HEK293 cells (Fig 2D). This effect was relatively small, and while it was reproduced by G $\beta$  $\gamma$  dialysis (Fig 3I), the effect of sumatriptan was not statistically significant on the inactivation time constant in DRG neurons (Fig 3F). This minor difference between HEK cells and DRG neurons may be caused by a number of factors, including potential auxiliary proteins present in DRG neurons but not in HEK cells, as well as differences in cell membrane mechanical properties or lipid composition.

### GABA<sub>B</sub> receptor activation inhibits Piezo1 currents via G $\beta$ $\gamma$

Our data show that Piezo2 currents are potentiated after activation of Gi-coupled receptors through a mechanism involving G $\beta$  $\gamma$ . However, vertebrates have two types of Piezo channels: Piezo1 and Piezo2. Piezo channels share about ~ 50% in protein sequence identity, possess similar biophysical properties, and are known to be similarly regulated by endogenous molecules [1,33,40,41]. Therefore, we tested whether the activation of Gi-coupled receptors could also affect the activity of Piezo1 channels. We transfected HEK293 cells with Piezo1 and GABA<sub>B</sub> receptors. We

recorded Piezo1 currents using a step protocol with increasing displacement of the mechanical probe, before and after application of baclofen. In contrast to Piezo2, activation of GABA<sub>B</sub> receptors by 25  $\mu$ M baclofen inhibited Piezo1 currents (Fig EV2A, B and D). This inhibition depended on activation of GABA<sub>B</sub> receptors because HEK293 cells transfected with only Piezo1 channels were not inhibited after baclofen treatment (Fig EV2E). Co-transfecting  $\beta$ ARKct abolished the inhibition of Piezo1 currents by activation of GABA<sub>B</sub> receptors (Fig EV2F), indicating that regulation of Piezo1 currents by activation of GABA<sub>B</sub> receptors was also mediated by G $\beta$  $\gamma$ .

Our data indicate that the Gi-signaling pathway is a general regulator of Piezo channels, but the regulatory mechanisms activated after receptor activation influence the activity of Piezo1 and Piezo2 differently. These findings have been in agreement with previous research showing that although Piezo1 and Piezo2 are closely related channels, they are expressed in different tissues [1] and possess different kinetics of inactivation [42], moderate cold temperatures inversely regulate their mechano-gated channel activity [43], and exogenous molecules are reported to selectively activate Piezo1 channels [44].

### PI3K and MAPK participate in potentiation of Piezo2 currents after activation of GABA<sub>B</sub> receptors

Figure 1B and F shows that the potentiation of MA currents lasted for several minutes, even after the removal of baclofen. G $\beta$  $\gamma$ -mediated effects on ion channel are usually quickly reversible; therefore, we tested whether G $\beta$  $\gamma$  modulated the activity of Piezo2 channels by a direct or indirect mechanism. We found that G $\beta$  $\gamma$  did not co-immunoprecipitate with either Piezo1 or Piezo2 channels, but showed clear co-immunoprecipitation with the G $\beta$  $\gamma$ -regulated Kir3.4 channels (Fig EV3), suggesting that G $\beta$  $\gamma$  may not be forming a complex with Piezo2 channels after activation of Gi-coupled receptors.

A potential mechanism of potentiation of Piezo2 currents could be the activation of protein kinases by G $\beta$  $\gamma$ . PI3K $\gamma$  and MAPK are downstream targets of G $\beta$  $\gamma$  [22,23]. These kinases have been associated with inflammatory hypersensitivity, NGF signaling, and inflammation in nociceptive neurons [45–47] and are possibly involved in affecting MA ion channels [48,49]. To test whether these kinases contribute to the potentiation of Piezo2 currents in HEK293 cells co-transfected with Piezo2 channels and GABA<sub>B</sub> receptors, we preincubated cells with the PI3K inhibitor wortmannin (50 nM) or with the MAPK inhibitor of U0126 (10  $\mu$ M). We measured Piezo2 currents using a step protocol with increasing displacement of the mechanical probe, before and after application of baclofen. Piezo2 currents measured in cells treated with either PI3K or MAPK inhibitors were not potentiated after activation of GABA<sub>B</sub> receptors, but Piezo2 currents in non-treated cells were potentiated (Fig 4A–C). These findings suggest that the prolonged potentiation of Piezo2 currents upon activation of Gi-coupled receptors is mediated by G $\beta$  $\gamma$ -downstream targets: PI3K and MAPK (Fig 4D).

PI3K activation was shown to increase surface expression of TRPV1 channels [46]; therefore, we also tested whether activation of GABA<sub>B</sub> receptors induces a change in Piezo2 surface expression using total internal reflection fluorescence (TIRF) microscopy. Figure EV4 shows that the plasma membrane fluorescence of the

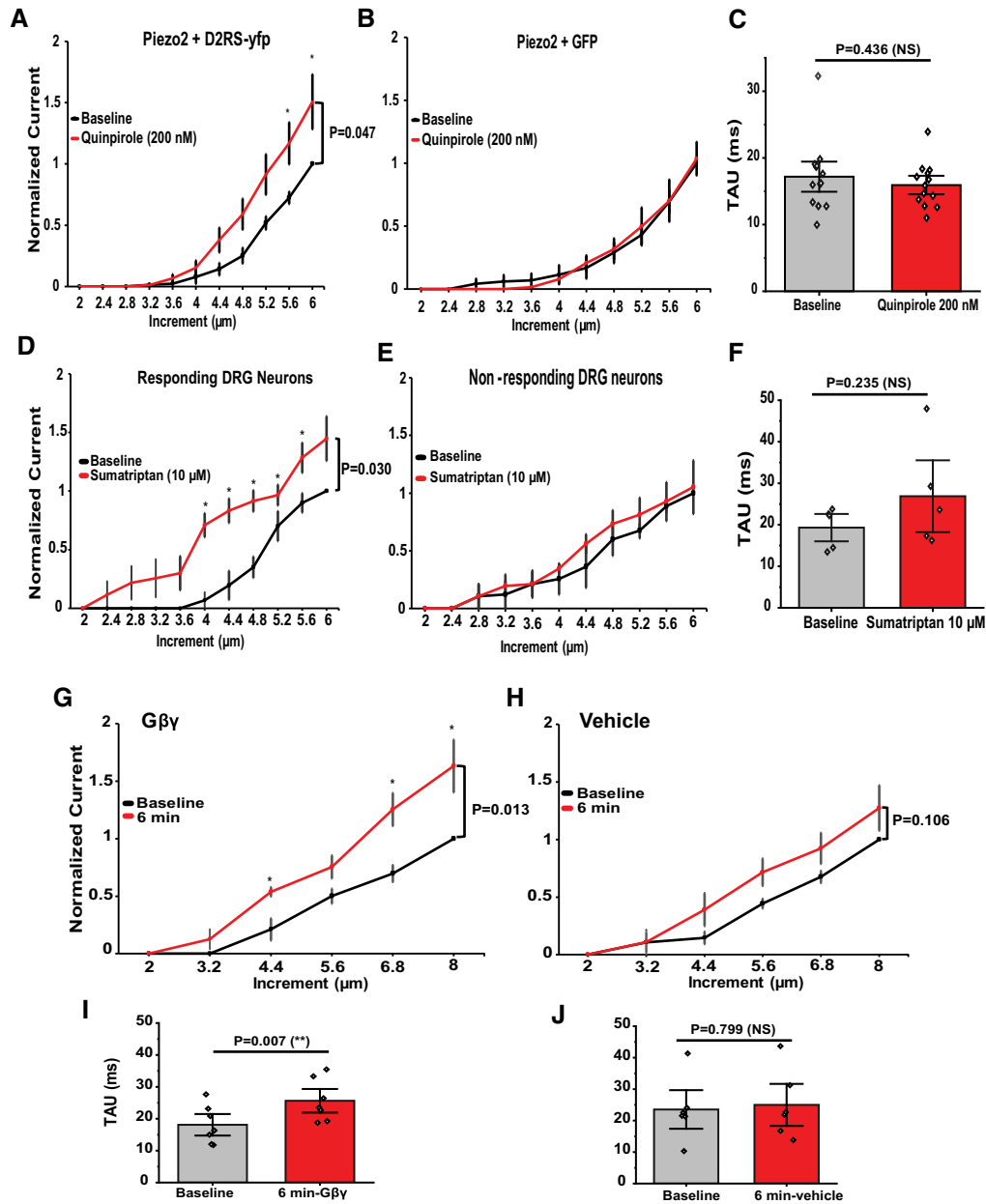


**Figure 3. Activation of other Gi-coupled receptors also potentiates native MA currents in DRG neurons and recombinant Piezo2 currents.**

- A, B Quantification of normalized MA Piezo2 currents in HEK293 cells transiently transfected with Piezo2 + D2RS-YFP (A,  $n = 13$ ) and HEK293 cells transfected with Piezo2 and GFP (B,  $n = 5$ ) before (black) and after (red) application of quinpirole 200 nM.  $*P < 0.05$ , repeated-measures ANOVA with Student's  $t$ -test no corrections. Data are shown as mean  $\pm$  SEM.
- C Quantification of Piezo2 current inactivation rate (Tau) in HEK cells transfected with Piezo2 + D2RS-YFP. Data are shown as mean  $\pm$  SEM and scatter plots ( $n = 13$ ).
- D, E Quantification of normalized MA currents in responding large DRG neurons (D,  $n = 5$ ) versus non-responding DRG neurons (E,  $n = 3$ ) before (black) and after (red) application of sumatriptan 10  $\mu\text{M}$  to activate the Gi-coupled Htr1d receptors.  $*P < 0.05$ , repeated-measures ANOVA with Student's  $t$ -test no corrections. Data are shown as mean  $\pm$  SEM.
- F Quantification of MA current inactivation rate (Tau) measured for responding (R) large DRG neurons ( $n = 5$ , paired  $t$ -test). Data are shown as mean  $\pm$  SEM and scatter plots.
- G, H Quantification of normalized MA currents recorded from large DRG neurons dialyzed with 50 ng/ml G $\beta\gamma$  (G,  $n = 7$ ) or with 0.0001% Lubrol (vehicle for G $\beta\gamma$ ; H,  $n = 6$ ).  $*P < 0.05$ , repeated-measures ANOVA with Student's  $t$ -test no corrections. Data are shown as mean  $\pm$  SEM.
- I, J Quantification of MA current inactivation rate (Tau) measured for large DRG neurons dialyzed with G $\beta\gamma$  ( $n = 7$ ,  $**P < 0.01$ , paired  $t$ -test) and vehicle (paired  $t$ -test). Data are shown as mean  $\pm$  SEM and scatter plots.

GFP-tagged Piezo2 did not change in response to baclofen application in HEK cells transfected with Piezo2-GFP and GABA<sub>B</sub> receptors, indicating that receptor activation did not increase trafficking of Piezo2 to the plasma membrane.

It was reported that PI(3,5)P<sub>2</sub>, a product of PI3K, positively regulates Piezo2 channels [31]. Due to lack of reliable specific probes for PI(3,5)P<sub>2</sub> [50], the involvement of this lipid in Piezo2 potentiation by Gi-coupled receptors is difficult to test, and wortmannin was reported to have only marginal effect on Piezo2 activity evoked by the knockdown of the myotubularin-related protein-2 (Mtmr2), a phosphatase enzyme that dephosphorylates PI(3,5)P<sub>2</sub> [31]. Further

experimentation and biochemical tools are needed to conclusively determine the mechanism of the involvement of PI3K and MAPK in regulating Piezo2 activity.

#### The serotonin 1B/1D agonist sumatriptan increases mechanosensitivity in mice via PI3K and MAPK

At the cellular level, our data show that activation of Gi-coupled receptors potentiates the activity of Piezo2 channels through an indirect mechanism involving the activation of Gβγ and its downstream targets PI3K and MAPK. To evaluate whether activation of

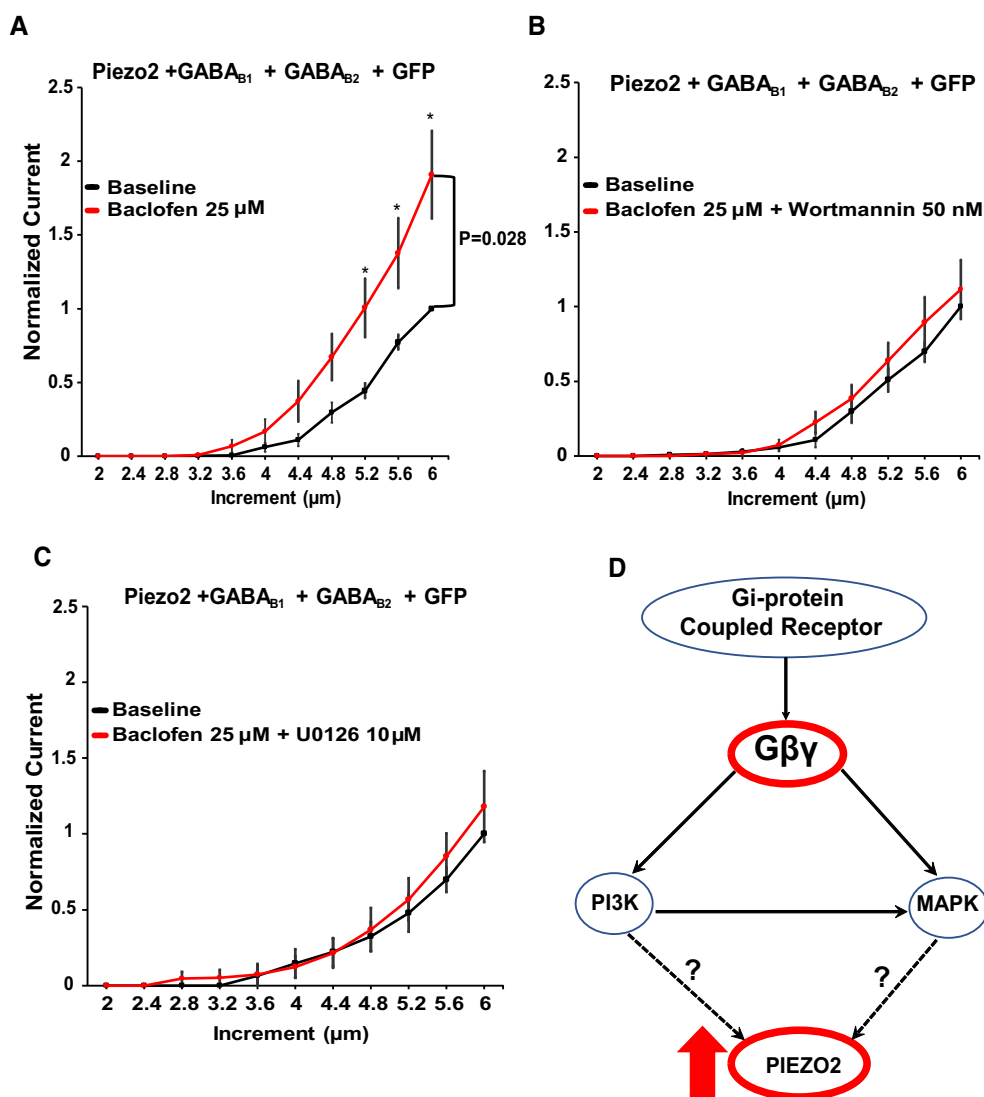


**Figure 4.** PI3K and MAPK participate in the potentiation of Piezo2 currents after activation of GABA<sub>B</sub> receptors.

A–C Quantification of normalized MA Piezo2 currents in HEK293 cells transiently transfected with Piezo2 + GABA<sub>B1</sub> + GABA<sub>B2</sub> + GFP (A,  $n = 12$ ), treated with the PI3K inhibitor wortmannin 50 nM (B,  $n = 10$ ) or treated with the MAPK inhibitor U0126 10 μM (C,  $n = 7$ ). \* $P < 0.05$ , repeated-measures ANOVA with Student's  $t$ -test no corrections. Data shown as mean  $\pm$  SEM. Cells were treated with wortmannin or U0126 for 30 min before the experiments and were present throughout the measurements.

D Putative pathway of regulation of Piezo2 currents by Gi-coupled receptors; activation of Gi-coupled receptors promotes the release of Gβγ activating PI3K and MAPK kinase, thus indirectly potentiating Piezo2 currents.

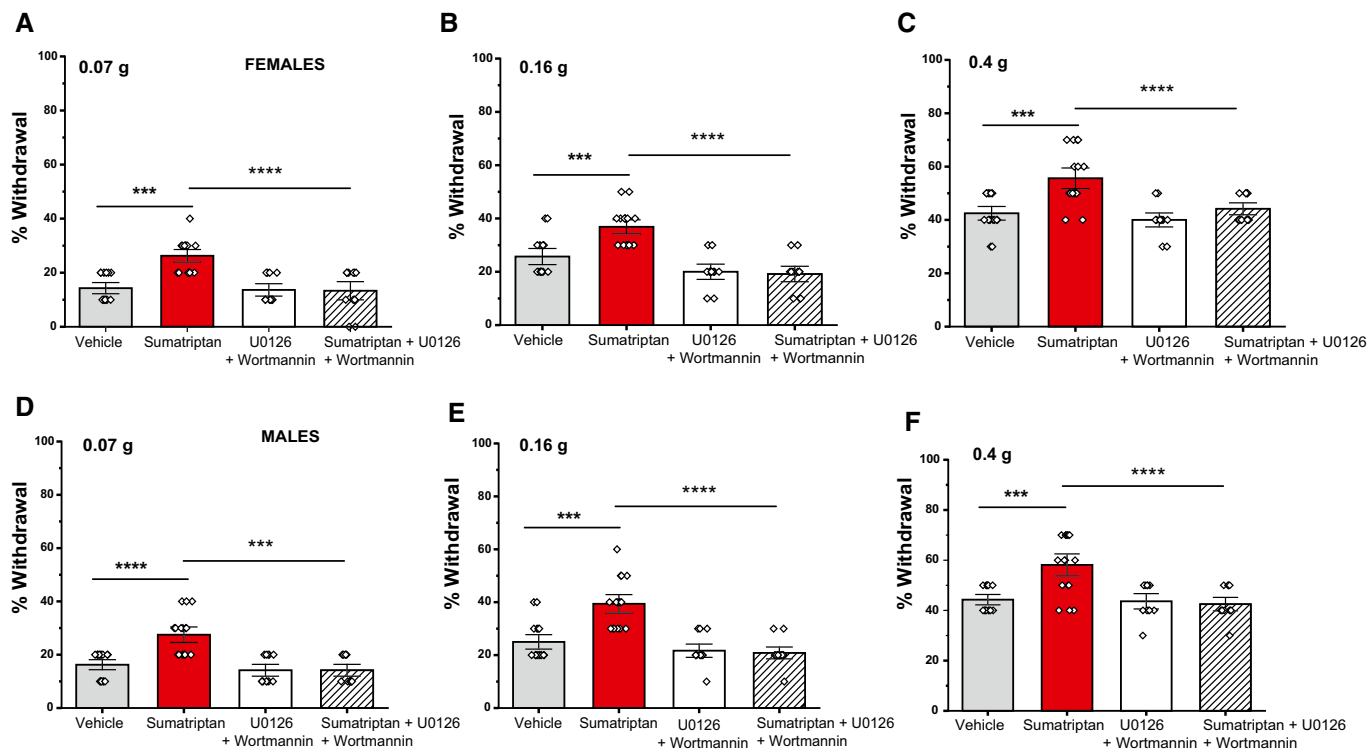


**Figure 5. Sumatriptan, the agonist of the Gi-coupled serotonin 1B/1D receptors, triggers mechanical hypersensitivity in mice via PI3K and MAPK.**

Mice were injected in the plantar surface of the hind paw with sumatriptan, or vehicle  $\pm$  the combination of wortmannin and U0126, as described in the Materials and Methods section. Mechanical sensitivity was assessed 30 min later using von Frey filaments in an ascending order.

A–C Percentage of withdrawal response for female mice using von Frey filaments at 0.07 g (A), 0.16 g (B), and 0.4 g (C) ( $n = 11$ –16 per group,  $***P < 0.001$ ,  $****P < 0.0001$ , one-way ANOVA with Tukey's multiple comparison test). Data are shown as mean  $\pm$  SEM and scatter plots.

D–F Percentage of withdrawal response for male mice using von Frey filaments at 0.07 g (D), 0.16 g (E), and 0.4 g (F) ( $n = 12$ –16 per group,  $***P < 0.001$ ,  $****P < 0.0001$ , one-way ANOVA with Tukey's multiple comparison test). Data are shown as mean  $\pm$  SEM and scatter plots.

Gi-coupled receptors could affect mechanosensitivity in mice, we performed experiments using von Frey filaments (0.07, 0.16, 0.4 g) to measure touch sensitivity, since responses to these filaments have been shown to be mediated by Piezo2 channels [3]. After intraplantar injection of sumatriptan, an agonist of the Gi-coupled Htr1b/Htr1d receptors, the frequency of withdrawal responses significantly increased to all filaments tested (Fig 5A–F). Moreover, this increase in mechanosensitivity was abolished in mice co-injected with sumatriptan and U0126 and wortmannin, an intervention that eliminated Piezo2 potentiation in our patch-clamp experiments. Our data indicate that activation of Gi-coupled receptors potentiates the activity of Piezo2 channels not only at the cellular level, but could also affect Piezo2-mediated peripheral processes such as touch sensitivity *in vivo* through an indirect PI3K/MAPK mechanism.

While activation of Gi-coupled receptors, such as opioid receptors, is generally associated with analgesia, it has also been documented that activation of Gi-coupled receptors may induce hyperalgesia and promote mechanical pain under certain circumstances [26–28]. While hyperalgesia usually requires repeated applications of Gi-coupled agonists, intradermal hind paw injection of the migraine drug sumatriptan evoked both an acute hyperalgesia 30 min after its injection, and hyperalgesic priming, potentiating the

effect of PGE2, an effect that developed several days after the injection of the drug [27]. The hyperalgesic effect of sumatriptan was proposed to play a role in migraine pain chronification in patients treated with this drug [27].

Sumatriptan has been described to have direct effects on other ion channels, such as inhibition of N-type  $Ca^{2+}$  channel [51], inhibition of voltage-gated  $Na^{+}$  channels [52], and inhibition of TRPV1 channels [53]. These effects, however, are unlikely to play a role in the electrophysiological or behavioral effects of sumatriptan in our study.

In conclusion, our data show that activation of Gi-coupled receptors potentiates Piezo2 and inhibits Piezo1 channel activity. This finding may be crucial when studying the Gi-signaling pathway of MA channels in different tissues with mechano-sensory properties. We also found that blocking the activity of  $G\beta\gamma$  abolished the potentiation and inhibition of Piezo currents. Additionally, our data also showed that  $G\beta\gamma$  may not be exerting its effect directly on Piezo2 channels, but potentially by activating its downstream targets: PI3K and MAPK, suggesting a possible non-canonical mechanism of action that could serve as source of investigation for understanding mechanical hyperalgesia induced by Gi-coupled receptor activation.



## Materials and Methods

### Cell culture

#### DRG neurons

All animal procedures were approved by the Institutional Animal Care and Use Committee at Rutgers NJMS. Mice were kept in a barrier facility under a 12/12-hr light–dark cycle, with the light cycle starting at 7 AM, a maximum of four mice were kept in the same cage, and they were not subjected to any procedure or drug administration before the experiments. Wild-type C57BL6 mice (2- to 4-month old) from either sex (Jackson laboratories) were anesthetized with i.p. injection of ketamine (100 mg/kg) and xylazine (12 mg/kg) and perfused via the left ventricle with ice-cold Hank's buffered salt solution (HBSS; Life Technologies). DRGs were harvested from all spinal segments after laminectomy and removal of the spinal column and maintained in ice-cold HBSS for the duration of the isolation. Isolated ganglia were cleaned from excess nerve tissue and incubated with type 1 collagenase (2 mg/ml; Worthington) and dispase (5 mg/ml; Sigma) in HBSS at 37°C for 30 min, followed by mechanical trituration. Digestive enzymes were then removed after centrifugation of the cells at 100 g for 5 min. Isolated DRG neurons were then resuspended and seeded onto glass coverslips coated with a mixture of poly-D-lysine (Life Technologies) and laminin (Sigma). DRG neurons were maintained in culture in Dulbecco's MEM/F12 (1:1) supplemented with 10% FBS (Thermo Scientific) and penicillin (100 IU/ml) and streptomycin (100 µg/ml; Life Technologies) for 16–48 h before measurements.

#### HEK293 cells

HEK293 cells were obtained from the American Type Culture Collection (ATCC; catalog number CRL-1573, RRID:CVCL\_0045) and were cultured in minimal essential medium (MEM; Life Technologies) containing 10% (v/v) HyClone characterized fetal bovine serum (FBS; Thermo Scientific), and penicillin (100 IU/ml) and streptomycin (100 µg/ml; Life Technologies). Cells were used up to 25–30 passages, when a new batch with low passage number was thawed. Cell was tested for mycoplasma contamination. Cells were transiently transfected at ~70–80% cell confluence with the Effectene reagent (QIAGEN) according to the manufacturer's protocol. Cells were then trypsinized and replated on poly-D-lysine-coated round coverslips 24 h after transfection. Fluorescent cells were subjected to electrophysiological measurements after 36–72 h. All cultured cells were kept in a humidity-controlled tissue-culture incubator with 5% CO<sub>2</sub> at 37°C.

### Whole-cell patch clamp electrophysiology

HEK293 cells were transiently transfected with the following cDNA constructs: mouse Piezo2 cloned into a pCMV-Sport6 vector (kind gift from Dr. Ardem Patapoutian), mouse Piezo2 tagged with GFP on its N-terminus, mouse Piezo1 cloned into a pcDNA 3.1 IRES GFP vector [1], human GABA<sub>B1</sub> receptor cloned into a pCMV-Sport6 vector, YFP-tagged GABA<sub>B1</sub> (kind gift from Dr. Stefano Marrullo) and GABA<sub>B2</sub> receptor cloned into a pcDNA 3.1 vector, rat βARK<sub>CT</sub> cloned into a mCherry2-C1 vector, human D2RS cloned into a EYFP-N2 vector (kind gift from Dr. Eldo Kuzhikandathil), and pEGFP-N1.

Whole-cell patch-clamp recordings were performed at room temperature (22–24°C) as described previously [54]. Briefly, patch

pipettes were prepared from borosilicate glass capillaries (Sutter Instrument) using a P-97 pipette puller (Sutter instrument) and had a resistance of 4–7 MΩ. After forming gigaohm-resistance seals, the whole-cell configuration was established, and the MA currents were measured at a holding voltage of -60 mV using an Axopatch 200B amplifier (Molecular Devices) and pCLAMP 10. Currents were filtered at 2 kHz using low-pass Bessel filter of the amplifier and digitized using a Digidata 1440 unit (Molecular Devices). All measurements were performed with extracellular (EC) solution containing 137 mM NaCl, 5 mM KCl, 1 mM MgCl<sub>2</sub>, 2 mM CaCl<sub>2</sub>, 10 mM HEPES, and 10 mM glucose (pH adjusted to 7.4 with NaOH). The patch pipette solution contained 140 mM K<sup>+</sup> gluconate, 1 mM MgCl<sub>2</sub>, 2 mM Na<sub>2</sub>ATP, 5 mM EGTA, and 10 mM HEPES (pH adjusted to 7.2 with KOH). In the case of intracellular dialysis of Gβγ to cultured DRG neurons, 50 ng/ml of Gβγ or equivalent lubrol (detergent in the vehicle for Gβγ; 0.0001%) was added to the patch pipette solution. The native Gβγ purified from bovine brain was purchased from MilliporeSigma.

Mechanically activated currents were measured from isolated DRG neurons or transiently transfected HEK293 cells as previously described [33]. Briefly, mechanical stimulation was performed using a heat-polished glass pipette (tip diameter, about 3 µm), controlled by a piezo-electric crystal drive (Physik Instrumente) positioned at 60° to the surface of the cover glass. The probe was positioned so that 10-µm movement did not visibly contact the cell but an 11.5-µm stimulus produced an observable membrane deflection. Two protocols were used to record the MA currents. For most experiments, we used a *step-increment protocol* when we applied an increasing series of mechanical steps from 12 µm in 0.4-µm increments every 15 s for a stimulus duration of 200 ms. Drugs were applied for 3 min, and then, the same protocol was repeated in the continuous presence of the drug. In the *continuous protocol* (Fig 1A and B), we used a fixed submaximal mechanical stimulus ranging from 5.2 to 7 µm (based on the step protocols for each cell) applied every 30 s for a stimulus duration of 200 ms. Measurements from cells that showed significant swelling after repetitive mechanical stimulation or had substantially increased leak current were discarded [55]. In the DRG neurons shown in Fig 1A, we measured the membrane potential, which was in the range of -50 to -60 mV, and did not change substantially from before the repetitive mechanical stimulation to the end of the experiment. The inactivation kinetics from MA currents were measured by fitting the MA current with an exponential decay function, which measured the inactivation time constant (Tau). To calculate this time constant, we used the current evoked by the third stimulation after the threshold in the incrementally increasing step protocol in most experiments, except in cells where only the two largest stimuli evoked a current. In the latter case, we used the current evoked by the largest stimulus, provided it reached 40 pA. Baclofen, carbachol, quinpirole, sumatriptan, and wortmannin were purchased from Sigma Aldrich and U0216 from Fisher Scientific.

### Behavioral testing

For von Frey experiments, male and female mice were acclimated in individual chambers for 30 min. After acclimation, intraplantar injection (10 µl) of either vehicle (3% DMSO in 0.9% NaCl) or sumatriptan (50 ng/paw), wortmannin (0.4 µg/paw), and U0126

(1 µg/paw) was performed, and 30 min later, mice were tested for touch sensitivity using the following filaments: 0.07, 0.16, and 0.4 g by stimulating the middle of plantar surface of the hind paw in an ascending order. The animals were randomly assigned to the experimental groups, and the experimenter was blinded to the drug injected. Each filament was presented 10 times, and the total percentage of withdrawal responses was scored per mouse.

### Co-immunoprecipitation

HEK293 cells on 6-well plates transfected with various constructs (indicated in Fig EV3) were harvested in lysis buffer (140 mM NaCl, 10 mM NaOH/HEPES, 50 mM Tris, 2.5 mM MgCl<sub>2</sub>, 1 mM EDTA, 1 mM EGTA, 0.5% Triton X-100) supplemented with protease and phosphatase inhibitor. Immunoprecipitation was performed by incubating pre-cleared cell lysates with primary anti-GFP antibody from Antibodies Inc (Anti-GFP clone N86/8 catalog# 75-131). The immune complex was incubated with pre-washed protein G agarose beads overnight at 4°C with gentle rocking. Immunoprecipitants were then used for Western blotting. After six washes, precipitates were eluted from the beads by incubating at 37°C for 1 h in Biorad XT loading buffer and XT reducing agent. Protein samples were run on 4–12% Bis-Tris Criterion gels and transferred to PVDF membranes. The membranes were blocked at room temperature in TBS-T with 5% milk for 1 hr and then probed overnight at 4°C with a rabbit polyclonal anti-Gβ antibody [56], recognizing Gβ1, Gβ2, Gβ3, and Gβ4 (T-20, SC-378; Santa Cruz) diluted 1:1,000 in TBS-T with 5% milk. Secondary antibody used was donkey-anti-rabbit HRP (Thermo Fisher, A16035) 1:5,000 in 5% Milk. For detecting GFP-tagged proteins in the input, we used an anti-GFP-HRP from Rockland Immunochemicals (catalog# 600-103-215). All blots were processed with SuperSignal West Pico Chemiluminescent Substrate (Thermo Fisher Scientific, Waltham, MA) and imaged with a Fuji Imager.

### Total internal reflection fluorescence imaging

HEK293 cells were transiently transfected with the following cDNA constructs: mouse Piezo2 tagged with GFP on its N-terminus, human GABA<sub>B1</sub> receptor cloned into a pCMV-Sport6, and GABA<sub>B2</sub> receptor cloned into a pcDNA 3.1 vector, or Pkdc1ab-GFP (DAG sensor) and the human M1 muscarinic receptor. Total internal reflection fluorescence measurements were performed as previously described [57], using an Olympus IX-81 inverted microscope equipped with an ORCA-FLASH 4.0 camera (Hamamatsu) and a single line TIRF illumination module. Excitation light was provided by 488 nm argon laser through a 60× NA 1.49 TIRF objective, and data were collected using the MetaMorph software (Molecular Devices). For experiments in Fig EV4, HEK293 cells were transfected with GFP-tagged Piezo2 with or without GABA<sub>B</sub>Rs or human muscarinic 1 (M1) receptors with the DAG sensor Pkdc1ab-GFP. Cells were plated on 25-mm glass coverslips, and solutions were manually applied to the chamber with gentle mixing. Data were analyzed using the MetaMorph and ImageJ softwares.

### Statistics

Data analysis was performed in Excel and SPSS. Data collection was randomized. No statistical method was used to predetermine

sample sizes, but our sample sizes are similar to those generally employed by the field. Data in most measurements were normalized by dividing every current value by the highest current value recorded from the baseline measurements of each cell before baclofen application. The normality of the data was verified with Shapiro–Wilk test. Data were analyzed with *t*-test, repeated-measures analysis of variance (ANOVA) with Student's *t*-test no corrections [58,59], or one-way ANOVA with Tukey's multiple comparison test. The *P* values are reported in the figure legends. Data are plotted as mean ± standard error of the mean (SEM) and scatter plots for most experiments.

**Expanded View** for this article is available online.

### Acknowledgements

T.R. was supported by NIH grants NS055159, GM093290, and GM131048; J.S.D.R. was supported by NIH grants F31NS100484 and F99NS113422, and T.M. by NIH grant GM111913. The authors thank Dr. Ardem Patapoutian (Scripps Research Institute) for providing us with the Piezo1 and Piezo2 clones, Dr. Stephano Marullo (Institut Cochin) for providing the myc-GABABR1-YFP clone, Dr. Eldo Kuzhikandathil (Rutgers Brain Health Institute) for providing the hD2RS-YFP clone, Dr. Diomedes Logothetis (Northeastern University) for providing the hM1 clone, and Dr. Tamas Balla (NIH) for providing the Pkdc1ab-GFP (DAG sensor).

### Author contributions

JSDR and TR designed the experiments. JSDR, YY, and SS performed experiments and data analysis. CH and TM performed and analyzed co-immunoprecipitation experiments. JSDR and TR wrote and edited the manuscript, TM, CH, YY, and SS edited the manuscript. TR provided funding and supervised the research study.

### Conflict of interest

The authors declare that they have no conflict of interest.

## References

- Coste B, Mathur J, Schmidt M, Earley TJ, Ranade S, Petrus MJ, Dubin AE, Patapoutian A (2010) Piezo1 and Piezo2 are essential components of distinct mechanically activated cation channels. *Science (New York, N.Y.)* 330: 55–60
- Alloui A, Zimmermann K, Mamet J, Duprat F, Noel J, Chemin J, Guy N, Blondeau N, Voilley N, Rubat-Coudert C *et al* (2006) TREK-1, a K<sup>+</sup> channel involved in polymodal pain perception. *EMBO J* 25: 2368–2376
- Ranade SS, Woo SH, Dubin AE, Moshourab RA, Wetzel C, Petrus M, Mathur J, Begay V, Coste B, Mainquist J *et al* (2014) Piezo2 is the major transducer of mechanical forces for touch sensation in mice. *Nature* 516: 121–125
- Woo SH, Lukacs V, de Nooij JC, Zaytseva D, Criddle CR, Francisco A, Jessell TM, Wilkinson KA, Patapoutian A (2015) Piezo2 is the principal mechanotransduction channel for proprioception. *Nat Neurosci* 18: 1756–1762
- Chesler AT, Szczot M, Bharucha-Goebel D, Ceko M, Donkervoort S, Laubacher C, Hayes LH, Alter K, Zampieri C, Stanley C *et al* (2016) The role of PIEZO2 in human mechanosensation. *N Engl J Med* 375: 1355–1364
- Szczot M, Liljencrantz J, Ghitani N, Barik A, Lam R, Thompson JH, Bharucha-Goebel D, Saade D, Necaie A, Donkervoort S *et al* (2018) PIEZO2

- mediates injury-induced tactile pain in mice and humans. *Sci Transl Med* 10: eaat9892
7. Murthy SE, Loud MC, Daou I, Marshall KL, Schwaller F, Kuhnemund J, Francisco AG, Keenan WT, Dubin AE, Lewin GR et al (2018) The mechanosensitive ion channel Piezo2 mediates sensitivity to mechanical pain in mice. *Sci Transl Med* 10: eaat9897
  8. Eijkelkamp N, Linley JE, Torres JM, Bee L, Dickenson AH, Gringhuis M, Minett MS, Hong GS, Lee E, Oh U et al (2013) A role for Piezo2 in EPAC1-dependent mechanical allodynia. *Nat Commun* 4: 1682
  9. Mahmud AA, Nahid NA, Nassif C, Sayeed MS, Ahmed MU, Parveen M, Khalil MI, Islam MM, Nahar Z, Rypens F et al (2017) Loss of the proprioception and touch sensation channel PIEZO2 in siblings with a progressive form of contractures. *Clin Genet* 91: 470–475
  10. Coste B, Houge G, Murray MF, Stitzel N, Bandell M, Giovanni MA, Philippakis A, Hoischen A, Riemer G, Steen U et al (2013) Gain-of-function mutations in the mechanically activated ion channel PIEZO2 cause a subtype of Distal Arthrogyriposis. *Proc Natl Acad Sci USA* 110: 4667–4672
  11. Alish F, Weichert A, Kalache K, Paradiso V, Longardt AC, Dame C, Hoffmann K, Horn D (2017) Familial Gordon syndrome associated with a PIEZO2 mutation. *Am J Med Genet A* 173: 254–259
  12. Nonomura K, Woo SH, Chang RB, Gillich A, Qiu Z, Francisco AG, Ranade SS, Liberles SD, Patapoutian A (2017) Piezo2 senses airway stretch and mediates lung inflation-induced apnoea. *Nature* 541: 176–181
  13. Zeng WZ, Marshall KL, Min S, Daou I, Chappleau MW, Abboud FM, Liberles SD, Patapoutian A (2018) PIEZO2s mediate neuronal sensing of blood pressure and the baroreceptor reflex. *Science (New York, N.Y.)* 362: 464–467
  14. Wu Z, Grillet N, Zhao B, Cunningham C, Harkins-Perry S, Coste B, Ranade S, Zebarjadi N, Beurg M, Fettiplace R et al (2017) Mechanosensory hair cells express two molecularly distinct mechanotransduction channels. *Nat Neurosci* 20: 24–33
  15. Feng J, Luo J, Yang P, Du J, Kim BS, Hu H (2018) Piezo2 channel-Merkel cell signaling modulates the conversion of touch to itch. *Science (New York, N.Y.)* 360: 530–533
  16. Dubin AE, Schmidt M, Mathur J, Petrus MJ, Xiao B, Coste B, Patapoutian A (2012) Inflammatory signals enhance piezo2-mediated mechanosensitive currents. *Cell Rep* 2: 511–517
  17. Robertson B, Taylor WR (1986) Effects of gamma-aminobutyric acid and (-)-baclofen on calcium and potassium currents in cat dorsal root ganglion neurones *in vitro*. *Br J Pharmacol* 89: 661–672
  18. Reuveny E, Slesinger PA, Inglese J, Morales JM, Iniguez-Lluhi JA, Lefkowitz RJ, Bourne HR, Jan YN, Jan LY (1994) Activation of the cloned muscarinic potassium channel by G protein beta gamma subunits. *Nature* 370: 143–146
  19. Badheka D, Yudin Y, Borbiro I, Hartle CM, Yazici A, Mirshahi T, Rohacs T (2017) Inhibition of transient receptor potential melastatin 3 ion channels by G-protein betagamma subunits. *eLife* 6: e26147
  20. Quallo T, Alkhatib O, Gentry C, Andersson DA, Bevan S (2017) G protein betagamma subunits inhibit TRPM3 ion channels in sensory neurons. *eLife* 6: e26138
  21. Dembla S, Behrendt M, Mohr F, Goecke C, Sondermann J, Schneider FM, Schmidt M, Stab J, Enzeroth R, Leitner MG et al (2017) Anti-nociceptive action of peripheral mu-opioid receptors by G-beta-gamma protein-mediated inhibition of TRPM3 channels. *eLife* 6: e26280
  22. Khan SM, Sleno R, Gora S, Zylbergold P, Laverdure JP, Labbe JC, Miller GJ, Hebert TE (2013) The expanding roles of Gbetagamma subunits in G protein-coupled receptor signaling and drug action. *Pharmacol Rev* 65: 545–577
  23. Clapham DE, Neer EJ (1997) G protein beta gamma subunits. *Annu Rev Pharmacol Toxicol* 37: 167–203
  24. Touhara K, Hawes BE, van Biesen T, Lefkowitz RJ (1995) G protein beta gamma subunits stimulate phosphorylation of Shc adapter protein. *Proc Natl Acad Sci USA* 92: 9284–9287
  25. Lopez-Illasaca M, Crespo P, Pellici PG, Gutkind JS, Wetzker R (1997) Linkage of G protein-coupled receptors to the MAPK signaling pathway through PI 3-kinase gamma. *Science (New York, N.Y.)* 275: 394–397
  26. Yudin Y, Rohacs T (2018) Inhibitory Gi/O-coupled receptors in somatosensory neurons: potential therapeutic targets for novel analgesics. *Mol Pain* 14: 1–16
  27. Araldi D, Ferrari LF, Levine JD (2016) Gi-protein-coupled 5-HT1B/D receptor agonist sumatriptan induces type I hyperalgesic priming. *Pain* 157: 1773–1782
  28. Araldi D, Ferrari LF, Levine JD (2018) Mu-opioid receptor (MOR) biased agonists induce biphasic dose-dependent hyperalgesia and analgesia, and hyperalgesic priming in the rat. *Neuroscience* 394: 60–71
  29. Thakur M, Crow M, Richards N, Davey GI, Levine E, Kelleher JH, Agle CC, Denk F, Harridge SD, McMahon SB (2014) Defining the nociceptor transcriptome. *Front Mol Neurosci* 7: 87
  30. Usoskin D, Furlan A, Islam S, Abdo H, Lonnerberg P, Lou D, Hjerling-Leffler J, Haeggstrom J, Kharchenko O, Kharchenko PV et al (2015) Unbiased classification of sensory neuron types by large-scale single-cell RNA sequencing. *Nat Neurosci* 18: 145–153
  31. Narayanan P, Hutte M, Kudryasheva G, Taberner FJ, Lechner SG, Rehfeldt F, Gomez-Varela D, Schmidt M (2018) Myotubularin related protein-2 and its phospholipid substrate PIP<sub>2</sub> control Piezo2-mediated mechanotransduction in peripheral sensory neurons. *eLife* 7: e32346
  32. Padgett CL, Slesinger PA (2010) GABA<sub>B</sub> receptor coupling to G-proteins and ion channels. *Adv Pharmacol* 58: 123–147
  33. Borbiro I, Badheka D, Rohacs T (2015) Activation of TRPV1 channels inhibits mechanosensitive Piezo channel activity by depleting membrane phosphoinositides. *Sci Signal* 8: ra15
  34. Szczot M, Pogorzala LA, Solinski HJ, Young L, Yee P, Le Pichon CE, Chesler AT, Hoon MA (2017) Cell-type-specific splicing of Piezo2 regulates mechanotransduction. *Cell Rep* 21: 2760–2771
  35. Wu J, Young M, Lewis AH, Martfeld AN, Kalmeta B, Grandl J (2017) Inactivation of mechanically activated Piezo1 ion channels is determined by the C-terminal extracellular domain and the inner pore helix. *Cell Rep* 21: 2357–2366
  36. Romero LO, Massey AE, Mata-Daboian AD, Sierra-Valdez FJ, Chauhan SC, Cordero-Morales JF, Vasquez V (2019) Dietary fatty acids fine-tune Piezo1 mechanical response. *Nat Commun* 10: 1200
  37. Logothetis DE, Kurachi Y, Galper J, Neer EJ, Clapham DE (1987) The beta gamma subunits of GTP-binding proteins activate the muscarinic K<sup>+</sup> channel in heart. *Nature* 325: 321–326
  38. Sato PY, Chuprun JK, Schwartz M, Koch WJ (2015) The evolving impact of G protein-coupled receptor kinases in cardiac health and disease. *Physiol Rev* 95: 377–404
  39. Hanack C, Moroni M, Lima WC, Wende H, Kirchner M, Adelfinger L, Schrenk-Siemens K, Tappe-Theodor A, Wetzler C, Kuich PH et al (2015) GABA blocks pathological but not acute TRPV1 pain signals. *Cell* 160: 759–770

40. Anderson EO, Schneider ER, Matson JD, Gracheva EO, Bagriantsev SN (2018) TMEM150C/Tentonin3 is a regulator of mechano-gated ion channels. *Cell Rep* 23: 701–708
41. Coste B, Murthy SE, Mathur J, Schmidt M, Mechioukhi Y, Delmas P, Patapoutian A (2015) Piezo1 ion channel pore properties are dictated by C-terminal region. *Nat Commun* 6: 7223
42. Soattin L, Fiore M, Gavazzo P, Viti F, Facci P, Raiteri R, Difato F, Pusch M, Vassalli M (2016) The biophysics of piezo1 and piezo2 mechanosensitive channels. *Biophys Chem* 208: 26–33
43. Zheng W, Nikolaev YA, Gracheva EO, Bagriantsev SN (2019) Piezo2 integrates mechanical and thermal cues in vertebrate mechanoreceptors. *Proc Natl Acad Sci* 116: 17547–17555
44. Syeda R, Xu J, Dubin AE, Coste B, Mathur J, Huynh T, Matzen J, Lao J, Tully DC, Engels IH et al (2015) Chemical activation of the mechanotransduction channel Piezo1. *eLife* 4: e07369
45. Obata K, Noguchi K (2004) MAPK activation in nociceptive neurons and pain hypersensitivity. *Life Sci* 74: 2643–2653
46. Zhang X, Huang J, McNaughton PA (2005) NGF rapidly increases membrane expression of TRPV1 heat-gated ion channels. *EMBO J* 24: 4211–4223
47. Leinders M, Koehn FJ, Bartok B, Boyle DL, Shubayev V, Kalcheva I, Yu NK, Park J, Kaang BK, Hefferan MP et al (2014) Differential distribution of PI3K isoforms in spinal cord and dorsal root ganglia: potential roles in acute inflammatory pain. *Pain* 155: 1150–1160
48. Dela Paz NG, Frangos JA (2019) Rapid flow-induced activation of Galphaq/11 is independent of Piezo1 activation. *Am J Physiol Cell Physiol* 316: C741–C752
49. Prato V, Taberner FJ, Hockley JRF, Callejo G, Arcourt A, Tazir B, Hammer L, Schad P, Heppenstall PA, Smith ES et al (2017) Functional and molecular characterization of mechanoinensitive “Silent” nociceptors. *Cell Rep* 21: 3102–3115
50. Hammond GR, Takasuga S, Sasaki T, Balla T (2015) The ML1Nx2 phosphatidylinositol 3,5-bisphosphate probe shows poor selectivity in cells. *PLoS ONE* 10: e0139957
51. Baillie LD, Ahn AH, Mulligan SJ (2012) Sumatriptan inhibition of N-type calcium channel mediated signaling in dural CGRP terminal fibres. *Neuropharmacology* 63: 362–367
52. Carbonara R, Carocci A, Roussel J, Crescenzo G, Buonavoglia C, Franchini C, Lentini G, Camerino DC, Desaphy JF (2015) Inhibition of voltage-gated sodium channels by sumatriptan bioisosteres. *Front Pharmacol* 6: 155
53. Evans MS, Cheng X, Jeffrey JA, Disney KE, Premkumar LS (2012) Sumatriptan inhibits TRPV1 channels in trigeminal neurons. *Headache* 52: 773–784
54. Yudin Y, Lukacs V, Cao C, Rohacs T (2011) Decrease in phosphatidylinositol 4,5-bisphosphate levels mediates desensitization of the cold sensor TRPM8 channels. *J Physiol* 589: 6007–6027
55. Hamill OP, McBride DW Jr (1997) Induced membrane hypo/hyper-mechanosensitivity: a limitation of patch-clamp recording. *Annu Rev Physiol* 59: 621–631
56. Mirshahi T, Robillard L, Zhang H, Hebert TE, Logothetis DE (2002) Gbeta residues that do not interact with Galpha underlie agonist-independent activity of K<sup>+</sup> channels. *J Biol Chem* 277: 7348–7355
57. Liu L, Yudin Y, Nagwekar J, Kang C, Shirokova N, Rohacs T (2019) Galphaq sensitizes TRPM8 to inhibition by PI(4,5)P2 depletion upon receptor activation. *J Neurosci* 39: 6067–6080
58. Jia Z, Ikeda R, Ling J, Gu JG (2013) GTP-dependent run-up of Piezo2-type mechanically activated currents in rat dorsal root ganglion neurons. *Molecular brain* 6: 57
59. Saville DJ (2003) Basic statistics and the inconsistency of multiple comparison procedures. *Can J Exp Psychol* 57: 167–175